Electromagnetic Induction by *Sq* Ionospheric Currents in a Heterogeneous Earth: Modeling Using Ground-based and Satellite Measurements

Jakub Velímský and Mark E. Everett

Department of Geology and Geophysics, Texas A&M University, College Station, TX 77843, USA. E-mail: `velimsky@geo.tamu.edu`

Summary: We have created a database consisting of hourly means of the geomagnetic field components observed on quiet days in years 2001–2002 on ground observatories, and Ørsted and CHAMP satellite measurements covering the same time intervals. In the first part of our study, we use the potential method to estimate the model of external inducing field. Following 3-D simulations are used to evaluate the effect of heterogeneous surface conductance map on Ørsted and CHAMP satellite measurements and to compare the results with observations. Improvement of up to 15% with respect to the best 1-D model was observed in surface observatory data as well as in the Ørsted and CHAMP measurements.
Keywords: electromagnetic induction, solar-quiet variations

1 Introduction

Effect of distribution of resistive continents and conductive oceans on electromagnetic induction in the Earth induced by daily variations of ionospheric currents (Sq) has been targeted by recent studies. Detailed study of the coastline effect on surface observatories was done in [3]. Authors of [1, 2] estimated the influence of near-surface heterogeneities at satellite altitudes. In the first part of our study, we use the potential method to estimate the model of external inducing field on selected quiet days in years 2001–2002. Following

3-D simulations are used to evaluate the EM induction signal on Ørsted and CHAMP satellites and compare the results with observations.

2 Data selection

Our study is based on data from three sources. The first dataset consists of the hourly mean values of magnetic induction vector from 126 permanent observatories provided by the World Data Center in Kyoto. The two other sources are the magnetic vector measurements by the CHAMP and Ørsted satellites sampled approximately at $1\,\mathrm{s}$. Following the discussion in [5], we limit ourselves to the Q^* quiet days. A day is denoted by Q^* when the sum of eight ap indices on this day, four ap indices on previous half-day, and four ap indices on following half-day does not exceed 60. There are 52 Q^* days in the period of interest 2001–2002.

Data from polar and equatorial observatories whose geomagnetic latitude is outside of the interval $5° \leq |\lambda_m| \leq 60°$ are excluded, since they are possibly affected by polar and equatorial jets. Data from the CHAMP and Ørsted satellites are resampled at $30\,\mathrm{s}$, polar and equatorial data points are excluded using the same criterion as in the case of surface observatories. We use the Ørsted model of geomagnetic field and its secular variation (OSVM, [4]) to remove the main field, the crustal field, the contribution of annual and semi-annual variations, and that of the magnetospheric ring current from the observatory and satellite data.

3 Harmonic analysis and 1-D inversion

The potential method is used to determine the inductive responses. We use the parameterization of magnetic potential by partial sums of products of spherical and time harmonics [5]. Namely,

$$U_1(r,\vartheta,\varphi;t) = 2\,a\,\mathcal{R}\left\{\sum_{p=1}^{P}\sum_{m=p-M}^{p+M}\sum_{j=m}^{m+J-1}\left[G_{jm,p}^{(e)}\left(\frac{r}{a}\right)^j + G_{jm,p}^{(i)}\left(\frac{a}{r}\right)^{j+1}\right]\right.$$

$$\left. P_{jm}(\cos\vartheta)\,e^{i\,m\,\varphi}\,e^{i\,\omega_p\,t}\right\}, \quad \text{for } a \leq r \leq a+h, \tag{1}$$

$$U_2(r,\vartheta,\varphi;t) = 2\,a\,\mathcal{R}\left\{\sum_{p,j,m}\left[-G_{jm,p}^{(e)}\frac{j}{j+1}\left(\frac{a+h}{a}\right)^{2j+1} + G_{jm,p}^{(i)}\right]\left(\frac{a}{r}\right)^{j+1}\right.$$

$$\left. P_{jm}(\cos\vartheta)\,e^{i\,m\,\varphi}\,e^{i\,\omega_p\,t}\right\}, \quad \text{for } r > a+h, \tag{2}$$

where $\mathcal{R}$ denotes the real part, r, ϑ, and φ are respectively the geocentric radius, colatitude, and longitude, $a = 6371.2\,\mathrm{km}$ is the Earth's radius, P_{jm} are the associated Legendre polynomials, and $\omega_p = 2\,\pi\,p\,\mathrm{rad/day}$ are the angular frequencies corresponding to the 1 day period and its harmonics. The limits of summation in (2) are the same as in (1). The ionosphere is assumed to be a thin layer of horizontal currents at altitude $h = 110\,\mathrm{km}$ above the surface. Therefore the magnetic field is expressed as $\boldsymbol{B}_\mathrm{S} = -\,\mathrm{grad}\,U_1|_{r=a}$ at the surface observatories and $\boldsymbol{B}_{\text{Ø},\mathrm{C}} = -\mathrm{grad}\,U_2$ at the Ørsted and CHAMP satellites. Note that potential U and the radial component of magnetic induction vector B_r change continuously across $r = a + h$. The series are truncated at $P = 6$, $M = 1$, and $J = 4$, yielding 72 complex coefficients of the external and internal field $G^{(e)}_{jm,p}$ and $G^{(i)}_{jm,p}$, respectively. The most stable terms are the principal terms $\left\{ G^{(e,i)}_{jm,p} \,\middle|\, j = p + 1,\ m = p \right\}$ which represent the largest part of local-time daily variations.

The initial intent was to find the harmonic coefficients $G^{(e,i)}_{jm,p}$ by fitting into the surface *and* the satellite data. However, preliminary results showed that the OSVM model failed to remove the non-Sq components of the field satisfactorily, leaving constant, or long-periodic baselines of amplitudes up to several hundreds nT on surface observatories. Similar results were obtained with the IGRF 2000 and CHAMP (CO2) models. Following [5], we removed the baselines from the surface data using the local midnight value for each Q^* day and each observatory. However, similar procedure is not possible with data observed by a moving satellite. Therefore we decided to use only the surface observatories in the spatio-temporal harmonic analysis. The satellite data are used in the next section for comparison of 3-D forward modeling results.

For each quiet day $k = 1, \ldots, 52$ in our database, we determined $G^{(e,i)}_{jm,p,k}$ by minimizing the misfit,

$$\chi^2_k\left(G^{(e,i)}_{jm,p,k}\right) = \sum_{l \in \mathcal{M}_k} \sum_{n=1}^{24} \left| \boldsymbol{B}_{\mathrm{S},ln} + \mathrm{grad}\,U_1(G^{(e,i)}_{jm,p,k}; a, \vartheta_l, \varphi_l; t_n) \right|^2, \qquad (3)$$

where index l runs through the set $\mathcal{M}_k$ of observatories available on the k-th day, $\boldsymbol{B}_{\mathrm{S},ln}$ is the n-th hourly value observed at the l-th observatory, and $t_n = (n - 1/2)\,\mathrm{h}$ UTC. The problem of minimization is solved using the singular-value decomposition technique.

Using the univariate linear regression analysis,

$$G^{(i)}_{jm,p,k} = q_{jm,p}\, G^{(e)}_{jm,p,k} + \delta G^{(i)}_{jm,p,k}, \quad k = 1, \ldots, 52, \qquad (4)$$

we find the response functions $q_{jm,p}$ [6]. Assuming spherically symmetric conductivity, and taking into account only the principal terms of the harmonic expansion, we invert the observatory-based responses $q_{jm,p}$ in terms of a layer of resistivity ρ^* and thickness z^* above a perfect conductor, see Fig. 1. The

same responses are also inverted using a three-layer model, which creates the basis for following 3-D modeling.
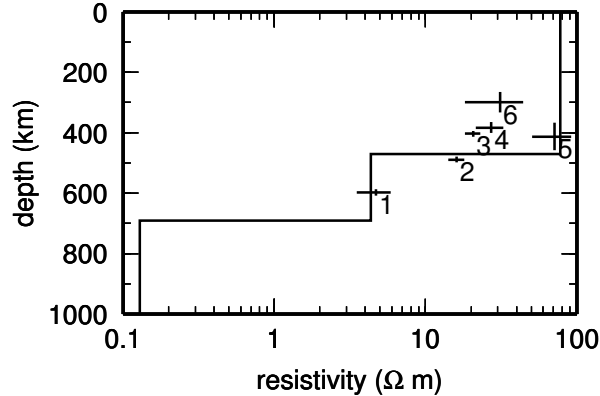

Fig. 1. Results of the 1-D inversion of observatory-based response functions. Crosses show the results of the inversion of principal spherical harmonic terms for time harmonics $p = 1, \ldots, 6$ in terms of a layer of resistivity ρ^* and thickness z^* above a perfect conductor. Error bars correspond to 68% level of confidence. The best-fitting three-layer model is shown by solid line

4 3-D forward modeling

In order to investigate the sensitivity of satellite data to the lateral conductivity heterogeneities in Sq-driven EM induction, we overlay the three-layer model derived in the previous section by the surface conductance map by [1]. Then, using the time-domain spherical harmonic-finite element approach [7], we excite the model by the external field coefficients $G^{(e)}_{jm,p,k}$ introduced above, and for each day we compute the time series of $\boldsymbol{B}$ on surface observatories and along the Ørsted and CHAMP trajectories. This is done separately for conductivity model without and with the conductance map, referenced respectively as 1-D and 3-D from now on.

Figure 2 shows the effect of the heterogeneous surface conductance map on observatories. We evaluate the total χ^2 misfit between the observed and modeled field over all 52 Q^* days at each station, separately for 1-D and 3-D models. The conductance map yields significantly better, up to 15% lower misfit on some coastal observatories, e.g. St. Johns (Newfoundland), Canberra (Australia), and most of the Japanese stations. On the other hand, some of the stations on the western African coast, San Juan in the Caribbean, and Trelew in South America, yield better results without the conductance map.
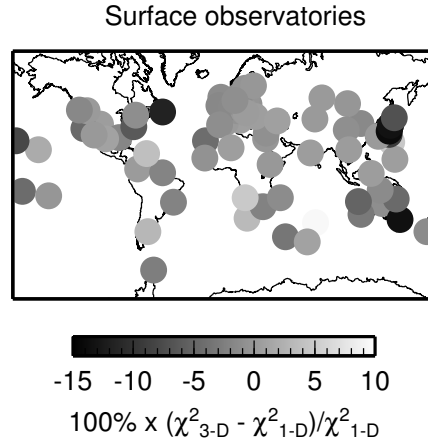
Surface observatories

$$100\% \times (\chi^2_{3\text{-D}} - \chi^2_{1\text{-D}})/\chi^2_{1\text{-D}}$$

Fig. 2. Relative improvement of the total misfit of data on surface observatories due to the surface conductance map

As expected, most of the continental stations in Eurasia are insensitive to the distant conductivity jumps across the coastlines.

Similar comparison is done using the satellite data. Local r^2 residua between observed and modeled 3-D and 1-D data are evaluated point-by-point along the satellite paths. Relative differences in residua are binned into $3° \times 3°$ bins and shown in Fig. 3 separately for Ørsted and CHAMP satellites. The results are similar to the surface observatories. Conductance map improves the fit to the data above the oceans by up to 15%. Smaller differences are observed above the continents far from the coastlines.
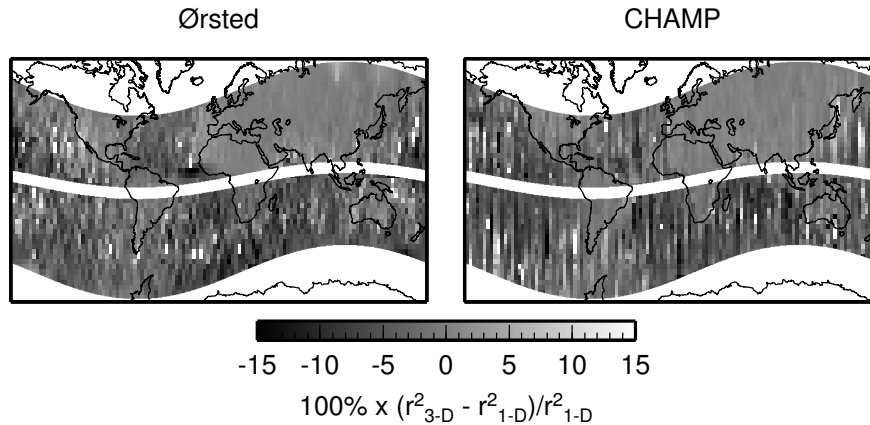
Ørsted   CHAMP

$$100\% \times (r^2_{3\text{-D}} - r^2_{1\text{-D}})/r^2_{1\text{-D}}$$

Fig. 3. Relative improvement of the residua due to the conductance map observed by the Ørsted and CHAMP satellites. The relative changes in residua are evaluated along the satellites paths and binned into $3° \times 3°$ bins

5 Conclusions

In the first part of our study we used the potential method [5, 6] with observatory data from period 2001–2002 and obtained similar results in terms of $\rho^*(z^*)$ (see Fig. 1 in [6]). The problem of removal of non-Sq signals from the satellite data prevented their use in the derivation of external Sq currents model. Further research to avoid this obstacle is highly desirable. The surface observatory-based, day-by-day model of ionospheric currents was used as input for 3-D modeling studying the influence of large conductance contrasts between oceans, continents and coastal shelves on surface observatory and satellite data. Our results confirm the importance of heterogeneous surface conductance in the EM induction modeling. Improvement of up to 15% with respect to the best 1-D model was observed in surface observatory data as well as in the Ørsted and CHAMP measurements. Satellite data acquired above oceans and coastal areas are highly sensitive to the conductance map. The differences between 1-D and 3-D solutions are much smaller above continents.

References

1. Everett, M.E., S. Constable, and C. Constable: Effects of near-surface conductance on global satellite induction responses. Geophys. J. Int., **153**, 277–286 (2003)
2. Grammatica, N. and P. Tarits: Contribution at satellite altitude of electromagnetically induced anomalies arising from a three-dimensional heterogeneously conducting Earth, using Sq as an inducing source field. Geophys. J. Int., **151**, 913–923 (2002).
3. Kuvshinov, A.V., D.B. Avdeev and O.V. Pankratov: Global induction by Sq and Dst sources in the presence of oceans: bimodal solutions for non-uniform spherical surface shells above radially symmetric earth models in comparison to observations. Geophys. J. Int., **137**, 630–650 (1999).
4. Olsen, N.: A model of the geomagnetic field and its secular variation for epoch 2000 estimated from Ørsted data. Geophys. J. Int., **149**, 454–462 (2002)
5. Schmucker, U.: A spherical harmonic analysis of solar daily variations in the years 1964–1965: response estimates and source fields for global induction — I. Methods. Geophys. J. Int., **136**, 439–454 (1999)
6. Schmucker, U.: A spherical harmonic analysis of solar daily variations in the years 1964–1965: response estimates and source fields for global induction — II. Results. Geophys. J. Int., **136**, 455–476 (1999)
7. Velímský, J.: Time-domain, spherical harmonic-finite element approach to transient three-dimensional geomagnetic induction in a spherical heterogeneous Earth. Submitted to Geophys. J. Int. (2003)